

Figure 1: Potential temperature isolines (contour interval 1 K, starting from 299.5 K) at $t = 900$ s for the density current test case with an 'Agnesi' hill (green color) on the left side of the domain.

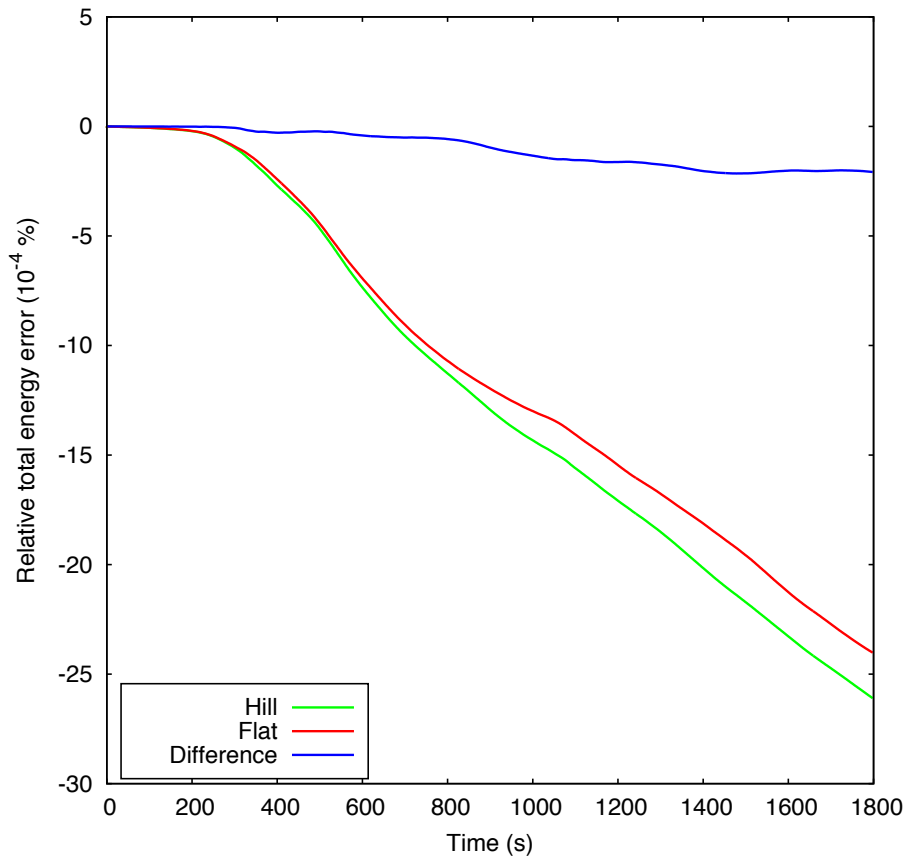


Figure 2: Time series of total energy error for the density current test case with and without the hill. The error is expressed as $10^{-4}\%$ of the total energy at the beginning of the simulation.

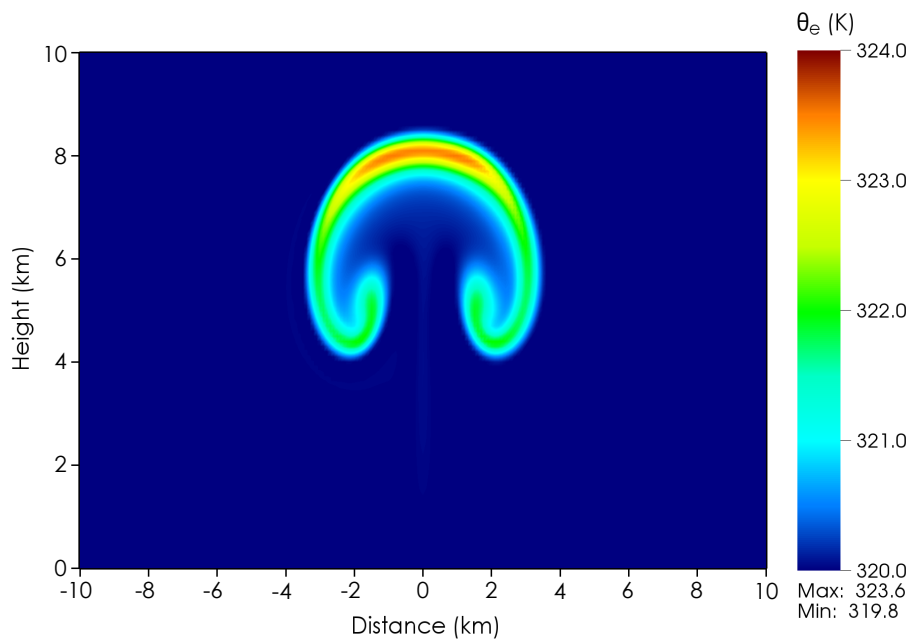


Figure 3: Equivalent potential temperature field for the moist rising bubble test case with background wind of $U = 20 \text{ m s}^{-1}$. Snapshot taken at $t = 1000 \text{ s}$ simulation time.

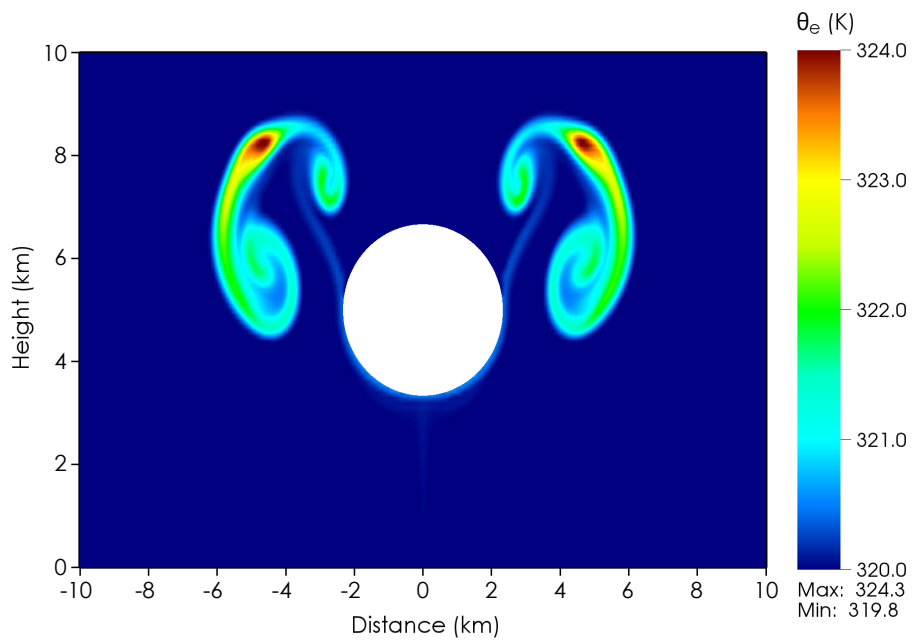


Figure 4: Equivalent potential temperature field for the moist rising bubble test including a zeppelin-shaped cut area in the center of the domain. Snapshot taken at $t = 1250$ s simulation time.

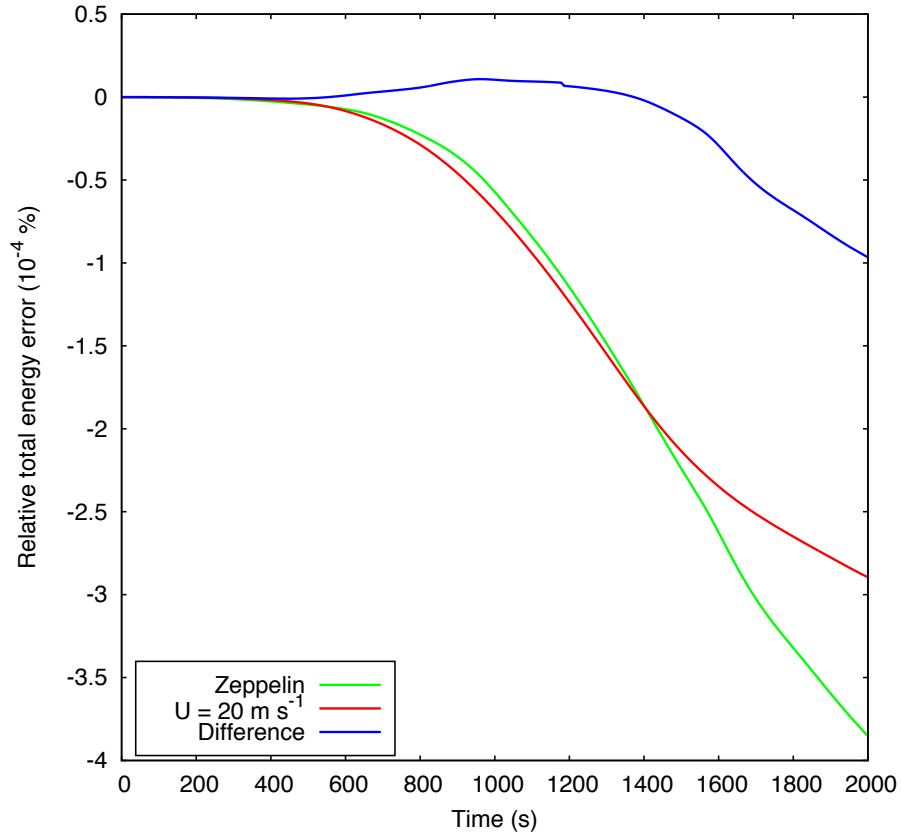


Figure 5: Same as Figure 2, but for the zeppelin and the lateral transported moist bubble test cases.

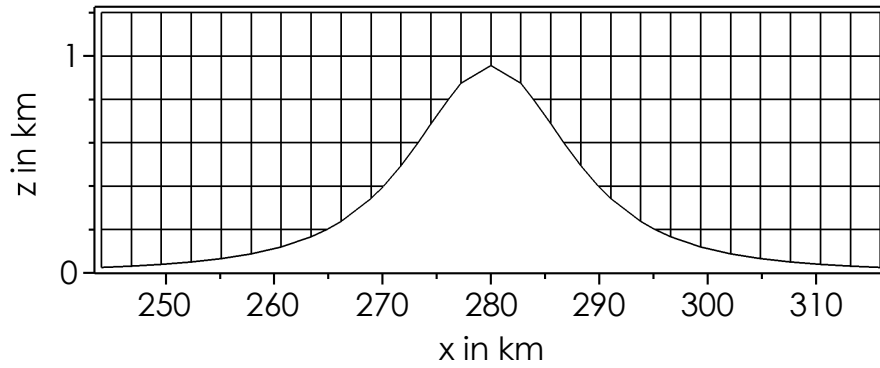


Figure 6: Computational grid around the mountain for an x - z cut plane at $y = 1.38$ km (cell center)

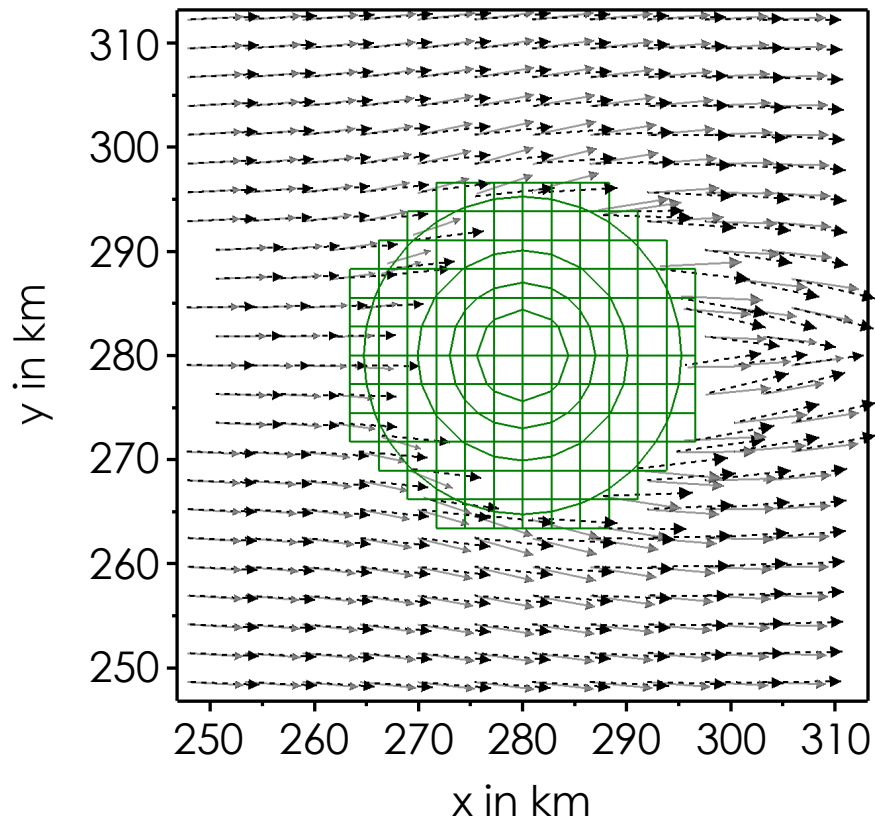


Figure 7: Horizontal cross-section of horizontal wind vectors at $z = 200$ m height for the RH95 case (black) and the RH50 case (grey). Surface grid cells around the mountain in green, circle lines represent 200 m orography intervals.

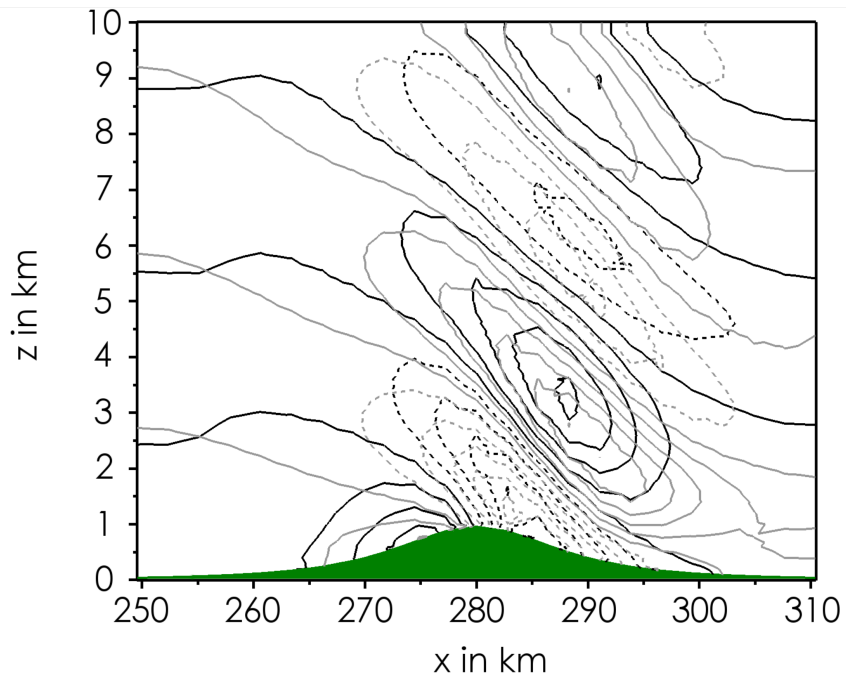


Figure 8: Vertical cross-section (x - z plane) of vertical wind speed for the RH95 case (black) and the RH50 case (grey). Updrafts in solid lines (0.2 m s^{-1} contour interval, zero line included), downdrafts in dashed lines (0.2 m s^{-1} contour interval, zero line excluded).

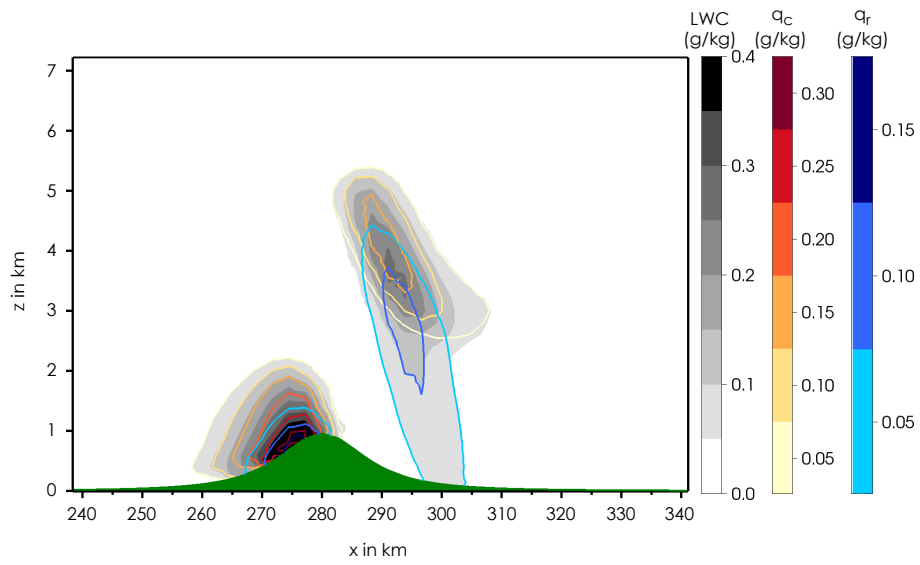


Figure 9: Vertical cross-section (x - z plane) of microphysical properties for the RH95 case. Liquid water content (shaded), contours of specific cloud water content q_c (red-yellow) and specific rain water content q_r (blue).